

Electric-field-induced optical second-harmonic generation in KTaO_3 and SrTiO_3

Y. Fujii and T. Sakudo

Electrotechnical Laboratory, Tanashi, Tokyo, Japan

(Received 2 September 1975)

Electric-field-induced optical second-harmonic generation (SHG) has been studied for KTaO_3 and SrTiO_3 in the temperature range from 300 to 4.2 K. The results can be summarized by the fourth-order Miller constants (in units of 10^{-11} esu): for KTaO_3 , $|\Delta_{111}| = 2.2 \pm 30\%$ and $|\Delta_{112}| = 0.77 \pm 33\%$; for SrTiO_3 , $|\Delta_{111}| = 0.56 \pm 34\%$ and $|\Delta_{112}| = 0.77 \pm 36\%$. The anisotropy of the SHG coefficients varies considerably among these isomorphous crystals: the ratios $|d_{33}/d_{31}|$ are $2.86 \pm 6\%$, $0.74 \pm 5\%$, and $0.37 \pm 15\%$ for KTaO_3 , SrTiO_3 , and BaTiO_3 , respectively. This is discussed in terms of Levine's bond-charge model of nonlinear optical susceptibilities.

I. INTRODUCTION

Recently, there has been considerable progress in understanding the microscopic mechanism of nonlinear optical properties. Theoretical analysis based on a bond-charge model has been especially successful in systematizing the optical second-harmonic-generation (SHG) coefficients of many AB compounds.^{1,2} There has also been a substantial effort to extend this theory to ferroelectric oxide crystals such as LiNbO_3 and BaTiO_3 .³

KTaO_3 and SrTiO_3 , isomorphous with BaTiO_3 , are paraelectric and nonpiezoelectric at all temperatures,⁴ but have dielectric constants as high as 10^4 at liquid-helium temperature.^{5,6} We have studied the effect of electric fields on their optical properties,^{7,8} with the viewpoint that these displacive-type ferroelectrics are best understood in terms of "spontaneous-polarization-induced" effects on the paraelectric "prototype" crystals. Previously, we have reported that the optical SHG was easily observable for SrTiO_3 and KTaO_3 when an external electric field was applied, and that the induced SHG coefficients were found to be proportional to the induced polarization.⁷

The electric-field-induced optical SHG is described by a fourth-rank tensor f_{ijkl} as⁹

$$P_i^{2\omega} = \sum_{jkl} f_{ijkl}^{2\omega 0 \omega \omega} E_j^0 E_k^\omega E_l^\omega, \quad (1)$$

where P_i and E_i denote, respectively, the i th components of an induced polarization and an electric field in the crystal ($i=1, 2, 3$: parallel to the pseudocubic $\langle 100 \rangle$ directions). Superscripts indicate the frequencies concerned. Experimentally, this effect is analyzed with a conventional SHG coefficient d_{ijk} which is related to f_{ijkl} by

$$d_{ijk}^{2\omega \omega \omega} = \sum_j f_{ijkl}^{2\omega 0 \omega \omega} E_j^0. \quad (2)$$

For highly polarizable materials such as KTaO_3 and SrTiO_3 , the electric field effect is better described as a function not of the external field but

of the local field which is proportional to the induced polarization. In this connection, it is useful to employ the fourth-order Miller constants Δ_{ijkl} defined by^{9,10}

$$\Delta_{ijkl} = (\chi_{ii}^{2\omega} \chi_{jj}^0 \chi_{kk}^\omega \chi_{ll}^\omega)^{-1} f_{ijkl}^{2\omega 0 \omega \omega}. \quad (3)$$

Using Δ_{ijkl} , Eq. (1) is transformed to

$$E_i^{2\omega} = \Delta_{ijkl} P_j^0 P_k^\omega P_l^\omega. \quad (4)$$

Experimental observations, to be described in Sec. III, show that the d_{ijk} are quite sensitive to temperature and to the bias-field strength, whereas the Δ_{ijkl} are not.

In a perovskite-type crystal biased along the pseudocubic $[001]$ direction, the ratio of the nonlinear coefficients (d_{33}/d_{31}) has an important bearing on the bond-charge theory. In this theory, we employ the following assumptions: (i) the macroscopic nonlinear optical susceptibility d_{ijk} may be

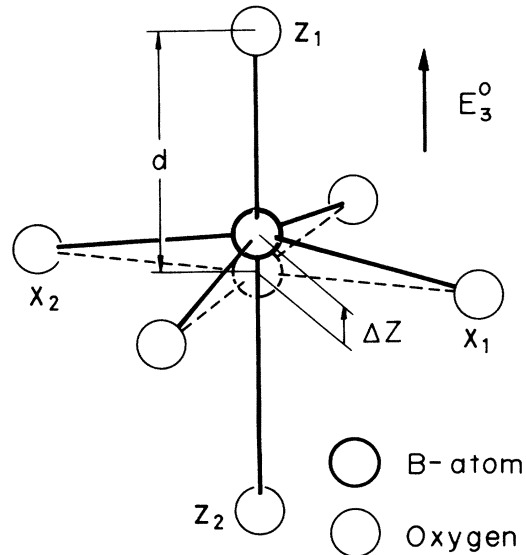


FIG. 1. $B-O_6$ octahedron in the ABO_3 perovskite-type crystals under a biasing electric field along the $[001]$ direction.

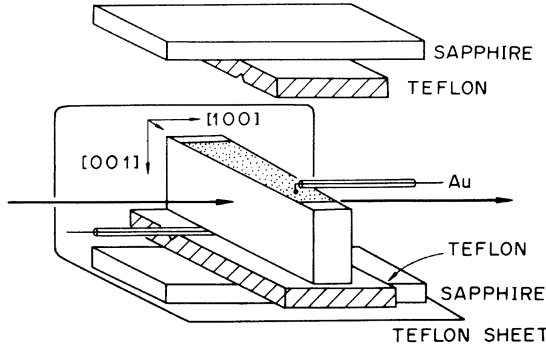


FIG. 2. Sample and insulating accessories. The electrodes are evaporated Al, ultrasonically welded with Au lines and covered with GE-7031 insulating varnish.

resolved into contributions from various types of bonds as^{2,11}

$$d_{ijk} = \sum_{\mu} G_{ijk}^{\mu} \beta^{\mu}, \quad (5)$$

where β^{μ} stands for the nonlinear optical polarizability of the μ th bond and G_{ijk}^{μ} is the bond geometrical factor; (ii) the nonlinear bond polarizability tensor is so highly anisotropic that the component transverse to the bond direction is negligible; (iii) contributions from the B-O bonds predominate over those from the A-O bonds (cf. Table I); and (iv) the dependence of β on the bond length d can be represented as a power law³

$$\beta \propto d^{\sigma_{NL}}. \quad (6)$$

We then get a particularly simple relation (for the derivation, see the Appendix and Fig. 1)

$$d_{33}/d_{31} = \sigma_{NL}, \quad (7)$$

irrespective of other details of the bond-charge theory. Hence, the experimental determination of the ratio d_{33}/d_{31} provides us with a chance to study the microscopic origin of the nonlinear optical phenomena in this type of crystal. Other aspects of the bond-charge theory will also be described in Sec. IV.

II. EXPERIMENTAL

The KTaO_3 crystal used in the experiment was grown by a top-seeded solution-growth method in our laboratory. The SrTiO_3 crystal was grown by a flame-fusion method at Nakazumi Crystals Corp. In order to employ the wedge technique for the Maker-fringe observation,¹² crystals were cut and polished to wedge shape, with dimensions of $2 \times 6 \times (1-2) \text{ mm}^3$ and with wedge angle of 10^{-2} – 10^{-3} rad. Each face except the inclined one was pseudo-cubic (100) plane. Electrodes were evaporated with aluminum on the $(1-2) \times 6\text{-mm}^2$ faces. Insulating accessories around the sample holder are

shown in Fig. 2.

The experimental arrangement is schematically shown in Fig. 3. An acoustically Q-switched YAG:Nd laser (transversely single mode, 100-mW average power, 100-cps pulse with 160-nsec width) was used as a fundamental light source. Half of the laser beam, divided by a splitter, was focused on a quartz crystal which emitted a reference SHG signal. The main beam was passed through a quarter-wave plate, a polarizer and filters, and focused by a lens ($f=100 \text{ mm}$) on the sample mounted at the holder in a cryostat. The cryostat temperature was controlled within $\pm 0.02^\circ \text{C}$ by the combination of a cold gas flow and a heater around the holder. For the Maker-fringe observation, the cryostat was set on a movable stage which was motor driven to move perpendicular to the laser beam at a rate of 0.1–0.2 mm/min. For biasing the sample, a high-power pulse generator supplied a voltage pulse, (up to 4 kV, 30- μsec duration) synchronized with the laser pulse.

SHG light beams generated from both the sample and the reference quartz were passed through ir-cut filters, analyzer, dielectric multilayer filters and ground-glass diffusers and were detected by cooled photomultipliers. These two signals were accumulated by boxcar integrators, and the value of the ratio was recorded. From the period of the recorded signal, the coherence length was obtained. Then, from the observed ratio of the average value of SHG power R , one can calculate the nonlinear coefficient of the sample (A) relative to that of quartz (B) with the relation¹²

$$\left| \frac{d_A}{d_B} \right| = \sqrt{R} \left(\frac{l_B}{l_A} \right) \left(\frac{n_A^{\omega} + 1}{n_B^{\omega} + 1} \right)^2 \left(\frac{n_A^{2\omega} + 1}{n_B^{2\omega} + 1} \right), \quad (8)$$

where l_A and n_A^{ω} are the coherence length and the refractive index of the sample (A), etc. In practice, over-all transmittance of the two optical paths and several other factors due to, e.g., multiple reflections at the sample surfaces were also

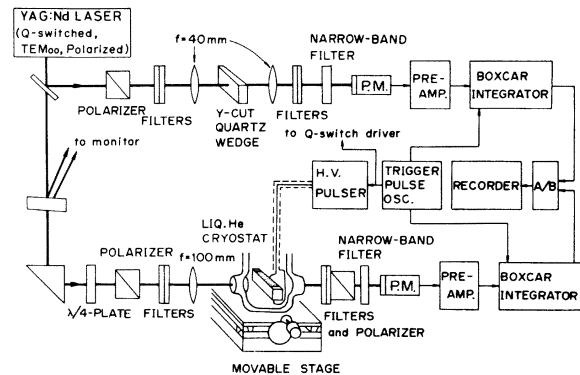


FIG. 3. Schematic diagram of experimental arrangement.

needed to be corrected for.

For observations of the electric field dependence and temperature characteristics, to be shown in Figs. 4 and 5, a different experimental arrangement using a Q-switched Nd-glass laser (10-MW peak power), a dc biasing voltage supply, oscilloscope recordings and the method of signal averaging with a wedge-shaped sample¹³ was employed.

III. RESULTS

A. KTaO₃

First, we examined the proportionality of the induced SHG coefficients and the corresponding polarization characteristics. Figures 4(a) and 4(b) show the electric field dependence of the nonlinear susceptibilities at 78 and 4.2 K, respectively. Lines in the figures represent the induced polarization P calculated from the observed dielectric constant¹⁴ $\epsilon(E)$ with the relation

$$P(E) = \frac{1}{4\pi} \int_0^E [\epsilon(E') - 1] dE'. \quad (9)$$

The temperature dependence of coefficients d_{33} and d_{31} under a constant biasing field is shown in Fig. 5. Each point in these figures represents the average of about ten measurements. Corresponding characteristics of the polarization are also shown for comparison. Except for a small extra contribution, to be explained in Refs. 15 and 16 the induced SHG susceptibilities were observed to vary concurrently with the electric polarization.

Next, using the arrangement described in the previous section, the magnitude of the induced SHG susceptibilities was carefully determined at 78 K and at 1.9 K. For this purpose, the value of the coherence length l_c of this crystal was measured by observing the periodicity of the Maker-fringe for the SHG signal at both temperatures to be

$$l_c = 2.77 \mu\text{m} \pm 2\%. \quad (10)$$

This agrees well with the value calculated from the linear susceptibilities at room temperature¹⁴ ($n^\omega = 2.171$ and $n^{2\omega} = 2.266$, which gives $l_c = 2.79 \mu\text{m}$). Then, from the SHG measurement at 78 K and at $E_3^0 = 20.5$ kV/cm, we obtained

$$\begin{aligned} |d_{33}| &= (2.4 \pm 7\%) d_{11}^{\text{quartz}} = (2.8 \pm 27\%) \times 10^{-9} \text{ esu}, \\ |d_{31}| &= (0.86 \pm 9\%) d_{11}^{\text{quartz}} = (1.0 \pm 29\%) \times 10^{-9} \text{ esu}, \quad (11) \\ |d_{33}/d_{31}| &= 2.70 \pm 4\%, \end{aligned}$$

and, from the measurement at 1.9 K and $E_3^0 = 15.3$ kV/cm, we obtained

$$\begin{aligned} |d_{33}| &= (6.2 \pm 8\%) d_{11}^{\text{quartz}} = (7.5 \pm 28\%) \times 10^{-9} \text{ esu}, \\ |d_{31}| &= (2.1 \pm 11\%) d_{11}^{\text{quartz}} = (2.5 \pm 31\%) \times 10^{-9} \text{ esu}, \quad (12) \end{aligned}$$

$$|d_{33}/d_{31}| = 3.03 \pm 4\%,$$

where we employed as the reference for the absolute value the recommended value for quartz $d_{11}^{\text{quartz}} = (1.20 \pm 20\%) \times 10^{-9}$ esu.¹⁷ Kleinman's condition $d_{31} = d_{15}$ was found to hold within the experimental accuracy of observation.¹⁸ We now evaluate the Miller constants, using¹⁹ Eq. (3) and the result of dielectric measurement.¹⁴ The observed third-rank SHG coefficients shown in Eqs. (11) and (12) can both be reduced, within experimental error, to the fourth-rank Miller constants

$$|\Delta_{1111}| = (2.2 \pm 30\%) \times 10^{-11} \text{ esu}, \quad (13)$$

$$|\Delta_{1122}| = (0.77 \pm 33\%) \times 10^{-11} \text{ esu},$$

which are thus found to be independent of temperature. The ratio of the constants is, ignoring the small variation of the ratio with temperature, equal to

$$\left| \frac{\Delta_{1111}}{\Delta_{1122}} \right| = \left| \frac{d_{33}}{d_{31}} \right| = 2.86 \pm 6\%. \quad (14)$$

Here, it is to be noted that the experimental accuracy of the ratio is much better than that of the separate components. This is of importance from a theoretical viewpoint described below.

B. SrTiO₃

For this crystal, we have shown in a previous report⁷ that the electric-field-induced optical SHG effect was easily observable. The magnitude of the d_{ijk} coefficients was found, except for an extra constant contribution, to be proportional to that of the induced polarization, even at lower temperatures where the P - E characteristics were highly nonlinear. Here we report the refinement of data for this crystal at 120 K well above the structural phase transition temperature.

The value of the coherence length determined from the Maker-fringe observation was

$$l_c = 1.98 \mu\text{m} \pm 3\%. \quad (15)$$

The difference between l_{33} and l_{31} due to the quadratic electro-optic effect was negligible and the value agrees well with the one calculated from refractive indices at room temperature²⁰ ($n^\omega = 2.313$ and $n^{2\omega} = 2.445$, which gives $l_c = 2.02 \mu\text{m}$). The SHG observation at 120 K and $E_3^0 = 20.5$ kV/cm indicated that

$$\begin{aligned} |d_{33}| &= (1.11 \pm 12\%) d_{11}^{\text{quartz}} = (1.3 \pm 32\%) \times 10^{-9} \text{ esu}, \\ |d_{31}| &= (1.51 \pm 14\%) d_{11}^{\text{quartz}} = (1.8 \pm 34\%) \times 10^{-9} \text{ esu}, \\ |d_{33}/d_{31}| &= 0.74 \pm 5\%. \quad (16) \end{aligned}$$

Kleinman's condition $d_{31} = d_{15}$ was also found to hold in this crystal. The Miller constants were eval-

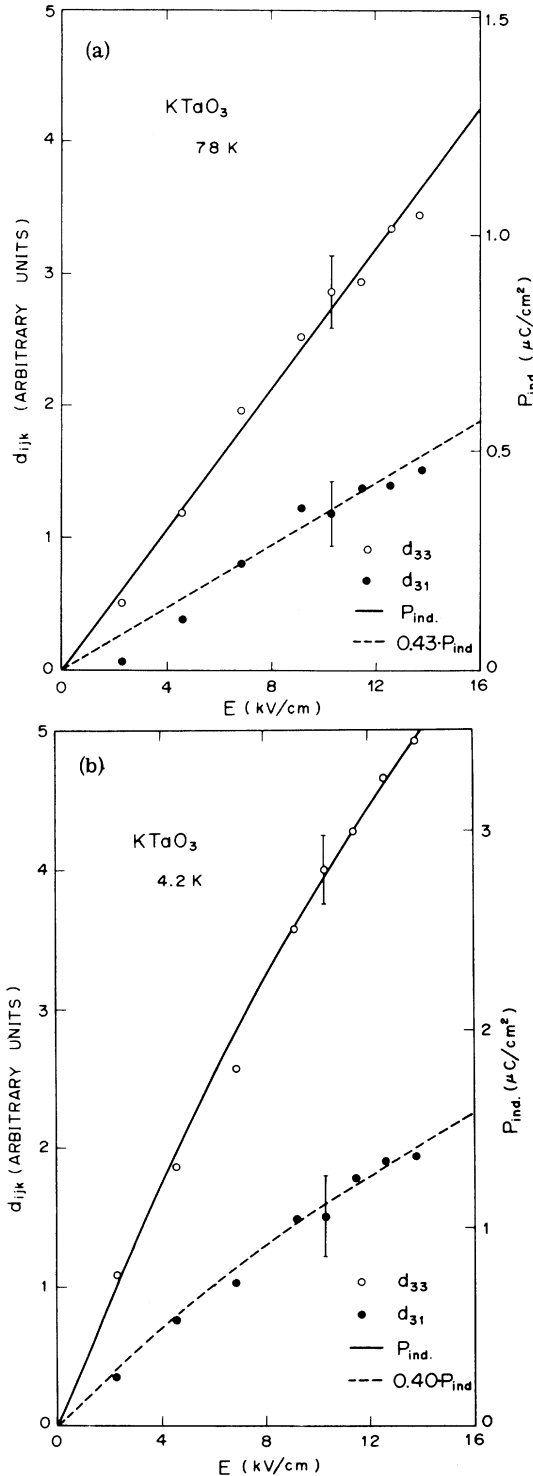


FIG. 4. Electric field dependences of d_{33} and d_{31} for KTaO_3 at (a) 78 K and at (b) 4.2 K. Experimental points in the figures represent averages of about ten measurements, and the bars show the typical standard errors. Residual intensity at zero-applied field is subtracted from the observed SHG intensity by the procedure explained in Ref. 15. Lines in the figures represent the observed characteristics of the induced polarization.

uated, using the corresponding dielectric data,⁶ as

$$\begin{aligned} |\Delta_{1111}| &= (0.56 \pm 34\%) \times 10^{-11} \text{ esu}, \\ |\Delta_{1122}| &= (0.77 \pm 36\%) \times 10^{-11} \text{ esu}. \end{aligned} \quad (17)$$

IV. DISCUSSION

First, let us comment briefly on the relative sign of d_{33} and d_{31} . Unfortunately, as the difference of coherence lengths (l_{33} and l_{31}) is very small, it was difficult to determine the relative sign in our case by the conventional interference method.²¹ For SrTiO_3 , the observation indicated that they were probably of the same sign. For KTaO_3 , it was not possible to determine the sign experimentally. Previously, Jerphagnon has studied the relation between the spontaneous polarization and the vector part v of the nonlinear susceptibility tensor,²² and found the empirical rule

$$v = -(1.0 \pm 0.3) \times 10^{-7} P_s \text{ esu}. \quad (18)$$

Applying this rule to the present case with Eqs. (2) and (3), we find the relation

$$\Delta_{1111} + 2\Delta_{1122} = -(3.3 \pm 1.0) \times 10^{-11} \text{ esu}. \quad (19)$$

Then, from the experimental data shown in Eqs. (13) and (14), we see that the values of $|\Delta_{1111} + 2\Delta_{1122}|$ should be (in units of 10^{-11} esu) 3.75 for KTaO_3 and 2.10 for SrTiO_3 if the sign is the same. On the other hand, if they are of different sign, they should be, respectively, 0.67 and 0.98. Hence, Jerphagnon's relation clearly favors for the same sign for d_{33} and d_{31} in both crystals.

Next, we compare the observed results with calculations based on the bond-charge theory. Following Levine's theoretical treatment of nonlinear optical susceptibility,^{2,3} we have evaluated various parameters to obtain the theoretical values of β and σ_{NL} for KTaO_3 and SrTiO_3 . The results are summarized, together with those for BaTiO_3

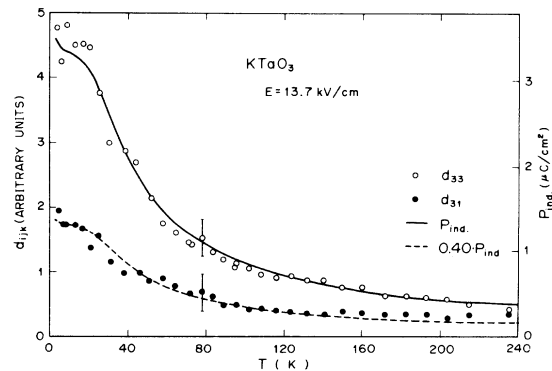


FIG. 5. Temperature dependences of d_{33} and d_{31} for KTaO_3 under $E = 13.7$ kV/cm. Lines are the corresponding characteristics of the induced polarization.

TABLE I. Theoretical parameters from the bond-charge theory, and the experimentally determined β and σ_{NL} ($=d_{33}/d_{31}$), for KTaO_3 , SrTiO_3 , and BaTiO_3 crystals.

	KTaO_3		SrTiO_3		BaTiO_3^a	
	K-O	Ta-O	Sr-O	Ti-O	Ba-O	Ti-O
$d^\mu(\text{\AA})^b$	2.82	2.00	2.76	1.95	2.81	2.00
$4\pi\chi^\mu$	2.22	6.34	2.05	8.36	2.41	7.74
$\chi_b^\mu(\text{\AA}^3)$	0.62	1.78 ^a	0.54	2.20 ^a	0.68	2.20
Z_α^*		5.9 ^a		7.1 ^a		7.1
$C^\mu(\text{eV})$	11.0	14.9	16.2	12.9	15.5	13.0
$E_h^\mu(\text{eV})$	3.0	7.2	3.2	7.6	3.1	7.1
f_i^μ	0.929	0.813	0.963	0.745	0.962	0.768
$\delta^\mu(10^{-28}\text{ esu})$	0.04	2.09	0.02	3.53	0.04	3.5
$\beta^\mu(10^{-30}\text{ esu})$	0.11	6.0	0.11	16.8	0.2	17
$\beta(\text{expt})(10^{-30}\text{ esu})$	$10.8 \pm 37\%$		$16.4 \pm 40\%$		$+21 \pm 28\%$	
σ_b^μ		+1.38		+0.37		+0.71
σ_{NL}^μ		-1.67		+1.43		+0.49
$\sigma_{NL}(\text{expt})$	$(\pm)2.86 \pm 6\%$		$(+)0.74 \pm 5\%$		$+0.37 \pm 15\%$	

^aSee Ref. 3.

^bF. Jona and G. Shirane, *Ferroelectric Crystals* (Pergamon, Oxford, 1962), Chap. V, p. 217.

for comparison, in Table I.

The outline of the bond-charge theory and the notations involved are described in the Appendix. To evaluate the linear susceptibilities, we adopted as optical refractive indices at the low-frequency limit $n=2.143$ for¹⁴ KTaO_3 and $n=2.270$ for SrTiO_3 .²⁰ The values of χ_b^μ for Ti-O and Ta-O bonds are estimated from the data of TiO_2 and LiTaO_3 .³ Z_α^* in Table I stands for the effective transition-metal core charge²³ which is assumed to be the same as Ti in TiO_2 and Ta in LiTaO_3 ,³ respectively. The β value was calculated using Eq. (A6), where the parameters involved were evaluated according to the bond-charge theory.^{2,3} The σ_{NL} value was calculated using Eq. (A8), where the parameter σ_b was evaluated using the empirical rule for the dependence of σ_b on f_i due to Levine³; for d -electron compounds,

$$\sigma_b = \begin{cases} 0 & (f_i < F_d), \\ 14.8(f_i - F_d) & (f_i > F_d), \end{cases} \quad (20)$$

where F_d represents a critical ionicity and is found to be 0.72. The experimental β values cited in the table were derived from the observed d_{31} values using Eq. (13) where the shift ΔZ of the B atom was estimated from the magnitude of polarization P assuming that ΔZ and P were proportional.²⁴

In the table, one notices the following: (i) the theoretical values of β^μ for the B-O bond are much larger than those of the A-O bond, which justifies the assumption that the contribution from the A-O bond may be neglected in evaluating σ_{NL} . (ii) The experimental values of β are found to be in fair agreement with theoretical ones, though the latter are a little smaller for KTaO_3 and BaTiO_3 . (iii) For the σ_{NL} values, there seems to be a substantial discrepancy between theory and experiment for both KTaO_3 and SrTiO_3 . Especially, the theory predicts a negative sign for σ_{NL} in KTaO_3 (i.e., a different sign for d_{33} and d_{31}), which contradicts Jerphagnon's rule (see above) and thus remains to be clarified experimentally.

Let us conclude with a comment on the observed disagreement for the σ_{NL} value. Within the framework of the bond-charge theory, it seems that, as the theoretical σ_{NL} is a sensitive function of f_i or σ_b [c.f. Eqs. (A7) and (A8)], a modification of the empirical relation of $\sigma_b - f_i$ expressed by Eq. (20) is needed. Or, it might suggest that some of the assumptions on which Eq. (7) is based are not warranted and need to be modified. Anyway, because of the theoretical importance of the parameter and the relatively high accuracy of the experimental determination of the ratio, this disagreement should not be simply overlooked but regarded as an interesting starting point for a further investigation of the mechanism of the non-

linear optical phenomena in this type of crystals.

ACKNOWLEDGMENTS

We would like to thank B. F. Levine for informing us of the details of his theoretical calculation, H. Unoki and H. Uwe for discussions, and K. Oka for growing KTaO_3 single crystals.

APPENDIX

To explain the notation used in the text (especially in Sec. IV and Table I), we now summarize the bond-charge theoretical treatment of nonlinear optical phenomena, mostly following Levine's papers.^{1,2,23} The theory is based on the following assumptions: (i) Charge in the bonding region in a crystal is weakly bound and highly mobile. Hence it is the main contributor to the linear and the nonlinear optical susceptibilities. The bond charge q is calculated as

$$(q/e) = n_v [1/\epsilon + (1/3)(1 - f_i)], \quad (\text{A1})$$

where n_v is the ratio of the number of s and p electrons to the number of bonds, ϵ is the low-frequency electronic dielectric constant, and f_i is the fractional ionicity (see below). (ii) The fractional ionicity of the bond can be determined by separating the average gap E_g into homopolar E_h and heteropolar C parts and then using

$$E_g^2 = E_h^2 + C^2, \quad (\text{A2})$$

$$f_i = C^2/E_g^2. \quad (\text{A3})$$

Expressions for E_g and E_h are given by

$$4\pi\chi = (\hbar\omega_p)^2 AD/E_g^2, \quad (\text{A4})$$

$$E_h = 39.74 d^{-s} \text{ (eV)}, \quad s = 2.48, \quad (\text{A5})$$

where χ is the low-frequency electronic susceptibility of the crystal, ω_p the plasmas frequency, A and D the correction factors (of order unity), and d is the bond length. For complex crystals composed of different bonds, these quantities must be specified for each type of bond (when necessary labelled by superscript μ).

One can then obtain the macroscopic nonlinear optical coefficient d_{ijk} from the constituent bond contributions β [cf. Eq. (5)]. The latter can be calculated, neglecting the homopolar contribution as in the case of BaTiO_3 ,³ by the theoretical expression

$$\begin{aligned} \beta &= (\chi^\omega)^2 \chi^{2\omega} \delta, \\ \delta &= \frac{600 b e^{-\hbar d/2} [Z_\alpha + (n/m)Z_\beta] \chi_b^2 C}{E_g^2 d^2 (q/e) \chi^3} \text{ esu}, \end{aligned} \quad (\text{A6})$$

where δ is the Miller constant, $e^{-\hbar d/2}$ the Thomas-Fermi screening factor, b the prescreening factor, Z_α and Z_β the numbers of valence electrons on the two bonding atoms (α and β), $n/m = \frac{3}{2}$ for ABO_3 compounds, and χ_b is the linear susceptibility of

a single bond.

The power-law exponent of the dependence of β on d is given by Eq. (6) in the text, or by

$$\sigma_{\text{NL}} \equiv \frac{d}{\beta} \frac{\partial \beta}{\partial d}. \quad (\text{A7})$$

By differentiating Eq. (A6), we get the expression

$$\sigma_{\text{NL}} = \sigma_0 - (6f_i - 2) \sigma_b, \quad (\text{A8})$$

where σ_b represents the power-law exponent of the prescreening factor b on d , and σ_0 is given by

$$\sigma_0 = (6s - \frac{1}{2}kd - 9) - [6(s - 1) - \frac{3}{2}kd]f_i. \quad (\text{A9})$$

These relations were used to calculate the σ_{NL} value cited in Table I.

If a crystal is composed of different types of bonds then the total electronic susceptibility χ may be resolved as

$$\chi = \sum_\mu F^\mu \chi^\mu = \sum_\mu N_b^\mu \chi_b^\mu, \quad (\text{A10})$$

where χ^μ is the total macroscopic susceptibility which a crystal composed entirely of bonds of type μ would have, F^μ the fraction of the μ th-type bond, χ_b^μ the single bond susceptibility, and N_b^μ is the number of bonds per cm^3 . For ABO_3 crystals,

$$\chi(\text{ABO}_3) = \frac{2}{3} \chi^{(\text{A-O})} + \frac{1}{3} \chi^{(\text{B-O})}. \quad (\text{A11})$$

Finally, we derive the important relation represented by Eq. (7). Consider the geometry of the B - O bonds in the perovskite-type crystal with the shift of B ion shown in Fig. 1, then, as G_{ijk} in Eq. (5) is simply a product of the direction cosines between the bond axes and the crystallographic axes, we can see that the d_{33} coefficient is mainly contributed from the B - $O(z_1)$ bond and the B - $O(z_2)$ bond, so called "the bond-stretching contribution,"² which may be calculated as follows:

$$\begin{aligned} d_{33} &= \sum_\mu G_{333}^\mu \beta^\mu \\ &= \frac{1}{V} \left[\left(\beta_0 - \frac{\partial \beta}{\partial d} \Delta Z \right) - \left(\beta_0 + \frac{\partial \beta}{\partial d} \Delta Z \right) \right] + O \left(\left(\frac{\Delta Z}{d} \right)^3 \right) \\ &= -\frac{2}{V} \left(\frac{\partial \beta}{\partial d} \right) \left(\frac{\Delta Z}{d} \right) \left(\frac{d}{\beta} \right) \beta_0 + O \left(\left(\frac{\Delta Z}{d} \right)^3 \right) \\ &\simeq -\frac{2}{V} \sigma_{\text{NL}} \left(\frac{\Delta Z}{d} \right) \beta_0. \end{aligned} \quad (\text{A12})$$

On the other hand, the d_{31} coefficient contributed by the B - $O(x_1)$ and the B - $O(x_2)$ bonds, so-called "the bond-bending contribution,"² is

$$d_{31} = -\frac{2}{V} \left(\frac{\Delta Z}{d} \right) \beta_0 + O \left(\left(\frac{\Delta Z}{d} \right)^3 \right).$$

Hence, we obtain the relation $d_{33}/d_{31} = \sigma_{\text{NL}}$. It should be remarked that this relation does not include β and so it should be possible to compare σ_{NL} and β independently with experiment.

- ¹Reference 2 includes an extensive collection of references in this area.
- ²B. F. Levine, Phys. Rev. B 7, 2600 (1973).
- ³B. F. Levine, Phys. Rev. B 10, 1655 (1974).
- ⁴R. A. Fleury and J. M. Worlock, Phys. Rev. 174, 613 (1968).
- ⁵S. H. Wemple, Phys. Rev. 137, A1575 (1965).
- ⁶T. Sakudo and H. Unoki, Phys. Rev. Lett. 26, 851 (1971).
- ⁷T. Sakudo and Y. Fujii, J. Phys. Soc. Jpn. Suppl. 28, 87 (1970). At that time, we employed the value $d_{ij}^{\text{quartz}} = 2.46 \times 10^{-9}$ esu which differs considerably from the value adopted in the present paper.
- ⁸Y. Fujii and T. Sakudo, J. Appl. Phys. 40, 720 (1969).
- ⁹F. N. H. Robinson, Bell. Syst. Tech. J. 46, 913 (1967).
- ¹⁰R. C. Miller, Appl. Phys. Lett. 5, 7 (1964).
- ¹¹C. R. Jeggo and G. D. Boyd, J. Appl. Phys. 41, 2741 (1970).
- ¹²G. D. Boyd, H. Kasper, and J. H. McFee, IEEE J. Quantum Electron. QE-7, 563 (1971).
- ¹³A. Savage, J. Appl. Phys. 36, 1496 (1965).
- ¹⁴Y. Fujii and T. Sakudo (unpublished).
- ¹⁵At zero-applied field a small residual SHG intensity I_0 was also observed amounting to, respectively, 3% and 0.6% of the observed SHG intensity $I^{\text{obs}}(E)$ for $E = 13, 7$ kV/cm at 78 and 4.2 K. We have tested two methods of subtracting the extra contribution: that is, $d_{ijk} \propto [I^{\text{obs}}(E) - I_0]^{1/2}$ under the out-of-phase condition and $d_{ijk} \propto [I^{\text{obs}}(E)]^{1/2} - I_0^{1/2}$ under the in-phase condition. The former procedure proved to give better fit with the polarization characteristics, the results of which are plotted in Fig. 4. As this effect is negligible for data in Fig. 5, no subtraction was done for the figure. This effect was previously reported for the case of electric-field-induced SHG in CaCO_3 (Ref. 16).
- ¹⁶R. W. Terhune, P. D. Maker, and C. M. Savage, Phys. Rev. Lett. 8, 404 (1962).
- ¹⁷R. Bechmann and S. K. Kurtz, *Landolt-Börnstein* (Springer-Verlag, Berlin, 1969), New Series, III-2.
- ¹⁸D. A. Kleinman, Phys. Rev. 126, 1977 (1962).
- ¹⁹For the case of nonlinear dielectrics as KTaO_3 and SrTiO_3 , the χ_{jj}^0 in Eq. (3) is not taken as the initial susceptibility but as the averaged one, as implied by Eq. (4).
- ²⁰M. Cardona, Phys. Rev. 140, A651 (1965).
- ²¹R. C. Miller and W. A. Nordland, Appl. Phys. Lett. 16, 174 (1970).
- ²²J. Jerphagnon, Phys. Rev. B 2, 1091 (1970).
- ²³B. F. Levine, Phys. Rev. B 7, 2591 (1973).
- ²⁴S. C. Abrahams, S. K. Kurtz, and P. B. Jamieson, Phys. Rev. 172, 551 (1968).